REPORT DOCUMENTATION PAGE

Form Approved
OMB No. 0704-0188

1. REPORT DATE *(DD-MM-YYYY)*	2. REPORT TYPE	3. DATES COVERED *(From - To)*
05-09-2005	REPRINT	

4. TITLE AND SUBTITLE
Tidal and Layer Structure in the Mesosphere and Lower Thermosphere

from TIMED/SABER CO_2 15-μm Emission

5a. CONTRACT NUMBER

5b. GRANT NUMBER

5c. PROGRAM ELEMENT NUMBER
62601F

6. AUTHOR(S)
R.H.Picard,[1] P.P. Wintersteiner,[2] J.R. Winick,[1] C.J. Mertens,[3] M.G.Mlynczak,[3]
J.M. Russell III,[4] L.L. Gordley,[5] W.E. Ward,[6] C.Y. She,[7] R.R. O'Neil[1]

5d. PROJECT NUMBER
2301

5e. TASK NUMBER
BD

5f. WORK UNIT NUMBER
A1

7. PERFORMING ORGANIZATION NAME(S) AND ADDRESS(ES)

Air Force Research Laboratory
29 Randolph Road
Hanscom AFB, MA 01731-3010

8. PERFORMING ORGANIZATION REPORT NUMBER

AFRL-VS-HA-TR-2005-1110

9. SPONSORING / MONITORING AGENCY NAME(S) AND ADDRESS(ES)

10. SPONSOR/MONITOR'S ACRONYM(S)

AFRL/VSBYB

11. SPONSOR/MONITOR'S REPORT NUMBER(S)

12. DISTRIBUTION / AVAILABILITY STATEMENT
Approved for Public Release; Distribution Unlimited.

[1]Air Force Research Laboratory, Hanscom AFB, MA
[2]ARCON Corporation, Waltham, MA
[3]NASA Langley Research Center, Hampton, VA
[4]Hampton University, Hampton, VA
[5]GATS, Inc., Newport News, VA
[6]University of New Brunswick, Fredericton, NB, Canada
[7]Colorado State University, Fort Collins, CO

13. SUPPLEMENTARY NOTES
Reprinted from: Remote Sensing of Clouds and the Atmosphere IX, Proceedings of SPIE Vol. 5571, Pages 182 - 192

14. ABSTRACT

The SABER radiometer on the TIMED spacecraft scans the earthlimb continuously in ten channels spanning the spectrum from 1.27 to 15 μm. The signature of the diurnal tide in the equatorial region is apparent throughout the mesosphere in TIME/SABER data, especially in the CO_2 15-μm radiance profiles. In addition, layer structures are apparent in a large fraction of the both the radiance profiles and the kinetic temperature profiles derived from them. We present results showing tidal and layer features in the variation with local time and latitude of 15-μm radiance and temperature. Temperature inversion layers (TILs) are regions of extreme perturbations in the retrieved temperature profile where the temperature increases rapidly over 3-10 km range by tens of degrees K, sometimes approaching increases of 100 K, and are not represented in any existing atmospheric climatologies. Theories that have been proposed connect them with the amplitude and phase of atmospheric tides, as well as with the interactions and dissipation of atmospheric gravity waves and planetary waves. The radiance local maxima, or "knees," are more mysterious. Their occurrence is rather unpredictable and not well explained by models, although it is known that they are due to vibrational excitation of CO_2 by atomic oxygen and they may have tidal connections. While they may be associated with strong TILs, the most important class occurring at tangent heights in the lower thermosphere between 100 and 115 km appear not to be simply related to local inversion layers. SABER data offers the opportunity to do the first global survey of MLT TLs, determine their spatial extent and persistence time, and develop a global climatology of their occurrence and properties.

15. SUBJECT TERMS
Earthlimb Infrared Atmospheric tides Temperature Inversion layers Radiance Layers

16. SECURITY CLASSIFICATION OF:			17. LIMITATION OF ABSTRACT	18. NUMBER OF PAGES	19a. NAME OF RESPONSIBLE PERSON
a. REPORT	b. ABSTRACT	c. THIS PAGE			Richard H. Picard
UNCLAS	UNCLAS	UNCLAS	SAR	11	19b. TELEPHONE NUMBER *(include area code)* 781-377-2222

Tidal and layer structure in the mesosphere and lower thermosphere from TIMED/SABER CO_2 15-μm emission

R. H. Picard,*[a] P.P. Wintersteiner,[b] J. R. Winick,[a] C. J. Mertens,[c] M.G. Mlynczak,[c]
J.M. Russell III,[d] L. L. Gordley,[e] W. E. Ward,[f] C. Y. She,[g] R. R. O'Neil[a]

[a]Air Force Research Laboratory, Space Vehicles Directorate, Hanscom AFB, MA 01731-3010, USA
[b]ARCON Corporation, 260 Bear Hill Road, Waltham, MA 02451, USA
[c]NASA Langley Research Center, Mail Stop 420, Hampton, VA 23681-2199, USA
[d]Hampton University, Center for Atmospheric Sciences, Hampton, VA 23668, USA
[e]GATS, Inc., 11864 Canon Blvd., Suite 101, Newport News, VA 23606, USA
[f]University of New Brunswick, Physics Dept., Fredericton, NB, Canada E3B 5A3
[g]Department of Physics, Colorado State University, Fort Collins, CO 80523-1875, USA

ABSTRACT

The SABER radiometer on the TIMED spacecraft scans the earthlimb continuously in ten channels spanning the spectrum from 1.27 to 15 μm. The signature of the diurnal tide in the equatorial region is apparent throughout the mesosphere in TIMED/SABER data, especially in the CO_2 15-μm radiance profiles. In addition, layer structures are apparent in a large fraction of the both the radiance profiles and the kinetic temperature profiles derived from them. We present results showing tidal and layer features in the variation with local time and latitude of 15-μm radiance and temperature. Temperature inversion layers (TILs) are regions of extreme perturbations in the retrieved temperature profile where the temperature increases rapidly over 3-10 km range by tens of degrees K, sometimes approaching increases of 100 K, and are not represented in any existing atmospheric climatologies. Theories that have been proposed connect them with the amplitude and phase of atmospheric tides, as well as with the interactions and dissipation of atmospheric gravity waves and planetary waves. The radiance local maxima, or "knees," are more mysterious. Their occurrence is rather unpredictable and not well explained by models, although it is known that they are due to vibrational excitation of CO_2 by atomic oxygen and they may have tidal connections. While they may be associated with strong TILs, the most important class occurring at tangent heights in the lower thermosphere between 100 and 115 km appear not to be simply related to local inversion layers. SABER data offers the opportunity to do the first global survey of MLT TILs, determine their spatial extent and persistence time, and develop a global climatology of their occurrence and properties.

Keywords: Earthimb, infrared, atmospheric tides, temperature inversion layers, radiance layers

1. INTRODUCTION

SABER[1] is a ten-channel radiometer, one of four instruments launched on 7 December 2001 aboard the TIMED spacecraft[2] into a 625-km circular orbit with an inclination of 74°. It scans the limb continuously from the hard earth up to almost 350 km tangent height (TH) using a moving mirror. The radiance data are oversampled, since they are spaced every 0.4 km in TH within SABER's 1.8-km field-of-view (FOV). TIMED's target region is the mesosphere and lower thermosphere (MLT) between altitudes of 60 and 180 km. SABER uses the channel radiances to derive atmospheric composition, kinetic temperatures (T_k), and heating / cooling rates. The three 15-μm CO_2 channels (channels 1-3) and the 4.3-μm CO_2 / NO^+ channel (channel 7) are used to derive T_k, pressure, and CO_2 volume mixing ratio (vmr) between

*richard.picard@hanscom.af.mil

Remote Sensing of Clouds and the Atmosphere IX, ed. Klaus P. Schäfer, Adolfo Comerón, Michel R. Carleer, Richard H. Picard, Nicolaos I. Sifakis, Proceedings of SPIE Vol. 5571 (SPIE, Bellingham, WA, 2004) · 0277-786X/04/$15 · doi: 10.1117/12.568060

15 and 130 km altitude.[3,4] The quality of the SABER temperature data has been validated by intercomparison with MacWAVE Campaign falling-sphere measurements[5], as well as lidar and other data.

The SABER instrument line-of-sight (LOS) looks at the earthlimb in a direction perpendicular to the satellite track. In the orbits of any given day, a specific local time (LT) is associated with all the measurements at any given latitude. However, as the TIMED orbit precesses slowly with a period near 64 d, the LT associated with a latitude changes through a large range. Moreover, the SABER instrument must always have its LOS on the antisunward side of the orbital plane in order to keep it from looking at the sun. Due to orbital precession this requires that a yaw maneuver be performed about every 64 days. The tangent points seen by the SABER instrument with a tangent height near 100 km altitude are located about 22° in earth-centered angle away from the sub-satellite points. The range of latitudes covered at the tangent point varies with the phase of the yaw cycle, alternating between 52S-84N and 84S-52N. Thus the coverage in the northern and southern hemispheres is asymmetrical, and high latitudes are fully accessible in only one hemisphere at a time.

The structure of the radiance and of the temperature as a function of LT and latitude reflects perturbations by a large number of atmospheric processes. Among the most important of these processes are atmospheric gravity waves (GWs) (for example[6-10]). GWs are typically launched by disturbances in the troposphere and propagate upward adiabatically while growing exponentially in amplitude in the linear regime. As their amplitude grows they undergo nonlinear interactions with other atmospheric modes or break and deposit their energy and momentum in the atmosphere affecting its energy budget. This coupling is especially efficient near critical layers where the horizontal phase speed of the wave equals the background horizontal wind in the direction of wave propagation.

Atmospheric tides[11] are special GWs whose period is a submultiple of the day. The most important ones, the migrating tides, are driven by solar heating in ozone and water vapor in the stratosphere and upper troposphere and are phase locked to the sun. The main periods present are 24 h (the diurnal tide, DT) and 12 h (the semidiurnal tide). Curiously, the GW wave vector is orthogonal to its group velocity, so that upward propagating GWs in the MLT from lower-atmospheric sources are associated with downward phase progression (and vice versa). This behavior applies equally to tides which, in the MLT above the forcing region, propagate downward with a vertical phase speed of one vertical wavelength (~ 22 km) in one tidal period, say 24 h. This amounts to a phase speed near 1km/hr.

Typical temperature and 15-μm radiance profiles show layer structures where the profiles reach local maxima. This is not in conformity with the overall trends in the MLT region for the temperature to reach a minimum at the mesopause height and for the radiance to decrease exponentially with TH. In the T_k profiles such temperature inversion layers (TILs) are often regions of extreme perturbations where the temperature increases rapidly over a 3-10 km range by several tens of degrees K, sometimes approaching increases of 100 K, and are not represented in any existing atmospheric climatologies. These inversions include peaks due to GW and tidal T_k oscillations, although their amplitudes are much larger than predicted by standard linear tidal models such as the GSWM.[12-14] Theories that have been proposed connect them with the amplitude and phase of atmospheric tides, as well as with the dissipation of atmospheric gravity waves and planetary waves and their nonlinear interactions with tides.[15-25] The radiance local maxima, or "knees," are more mysterious. Their occurrence is rather unpredictable and not well explained by models,[26-28] although it is known that they are due to vibrational excitation of CO_2 by atomic oxygen and they may have tidal connections. While they are sometimes associated with strong TILs,. the most important class occurring at THs in the lower thermosphere between 100 and 115 km appear to have no connection with local inversion layers.

In Section 2 we consider tidal effects in the SABER 15-μm radiance and T_k, following with a global survey of radiance and inversion layers in the SABER data. in Section 3 and the conclusions of the study in Section 4.

2. ASCENDING/DESCENDING DIFFERENCES AND TIDAL EFFECTS IN SABER CO_2 15-μM DATA

A survey of SABER Level 1B (calibrated channel radiance) data that was conducted early in the mission, as a part of the data validation process, revealed out-of-phase wavelike patterns in the ascending and descending CO_2 15-μm

(channel 1, 2, and 3) radiance that are strongly suggestive of DT oscillations, especially in the equatorial region. This led to an investigation of the associated non-LTE retrieved temperatures, which also showed tidal features.
At equatorial latitudes, we found that the daily mean radiance profiles for ascending and descending portions of the orbits differed by as much as 40% between 70 and 110 km TH, with the difference changing sign in an oscillatory manner. Oscillatory patterns were seen with a smaller amplitude at lower altitudes down to ~30 km. The natural interpretation is that the 15-μm emission rate directly reflects wavelike T_k and minor-species density oscillations in the atmosphere. These, in turn, are manifestations of atmospheric tides---particularly the DT---which dominates at low latitudes and produces the ascending/descending contrasts. Otherwise stated, the T_k oscillations arise from adiabatic tidal vertical displacements, which also modulate the atmospheric total density and the density of all minor constituents. This modulation of the constituent densities also contributes to the associated radiance oscillations.

These radiance difference patterns are present throughout the period we examined, and they vary in a striking way as the orbit precesses in local time. Figure 1 shows data from a 33-day period (21 Mar - 23 Apr 2002) within a single yaw cycle, during which the orbital precession produced a local-time change of ~6.5 hours. The difference profiles, taken for ten days distributed within this period, are characterized by tidal behavior[11] -- an amplitude that grows exponentially throughout the mesosphere, a vertical wavelength of ~22-25 km, and phase fronts descending with increasing local time at a rate of ~22 km/day. This vertical wavelength and vertical phase speed result in a period of 24 hr, exactly as expected for the DT. The radiance differences in Figure 1 are plotted as a fraction of the mean and offset from one another for clarity. Similar tidal patterns have been predicted and observed in airglow data.[29-32]

The ascending/descending LT difference is only ~8.8 hours at the equator, so the full amplitude of the tide is not manifest in any single day's data. At higher latitudes, where the semidiurnal tide is dominant, the radiance differences produce more complicated patterns, as one would expect. Nevertheless, they will also provide a useful means of studying tidal fluctuations.

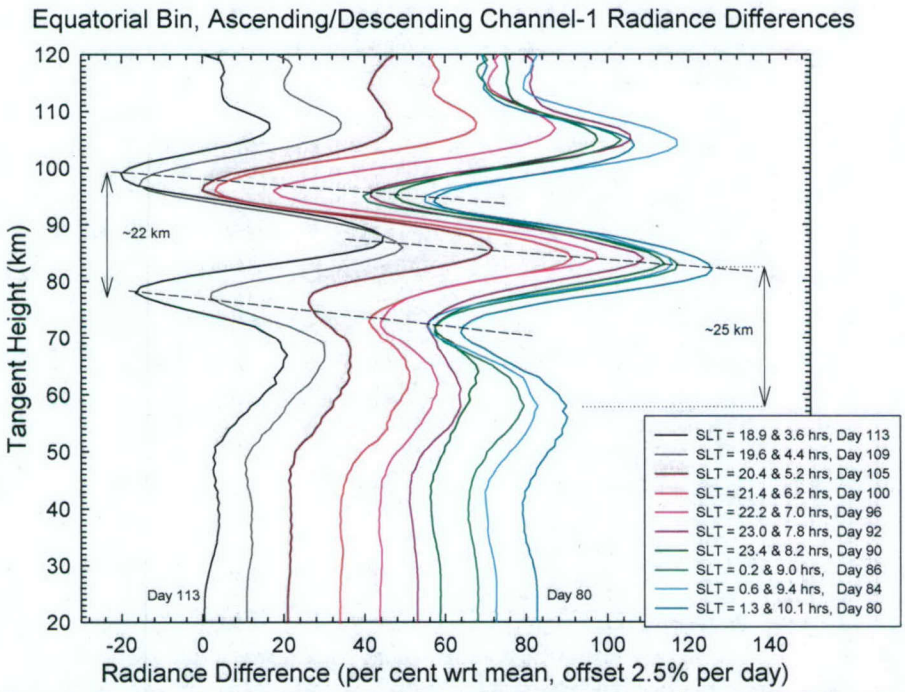

Figure 1. Compilation of SABER equatorial ascending/descending 15-μm radiance differences, corresponding to pairs of local times separated by ~8.8 hours, for ten days spaced throughout a 33-day period in March-April 2002. The data are characterized by a vertical wavelength of 22-25 km, a growing amplitude with tangent height, and phase fronts descending with increasing local time at a rate of ~22 km/day---all characteristics of the diurnal tide.

The DT signature is also obvious in the ascending/descending differences of retrieved T_k (Level 2A) data. In Figure 2 we show the modulation of the MLT temperature by the tide. The daily mean retrieved temperature at the equator is plotted for a typical day in late March 2002, separated into ascending/descending categories. As expected, both from the behavior of the radiance and from tidal theory, the difference profile has an exponentially growing amplitude and a wavelength of ~22-25 km.

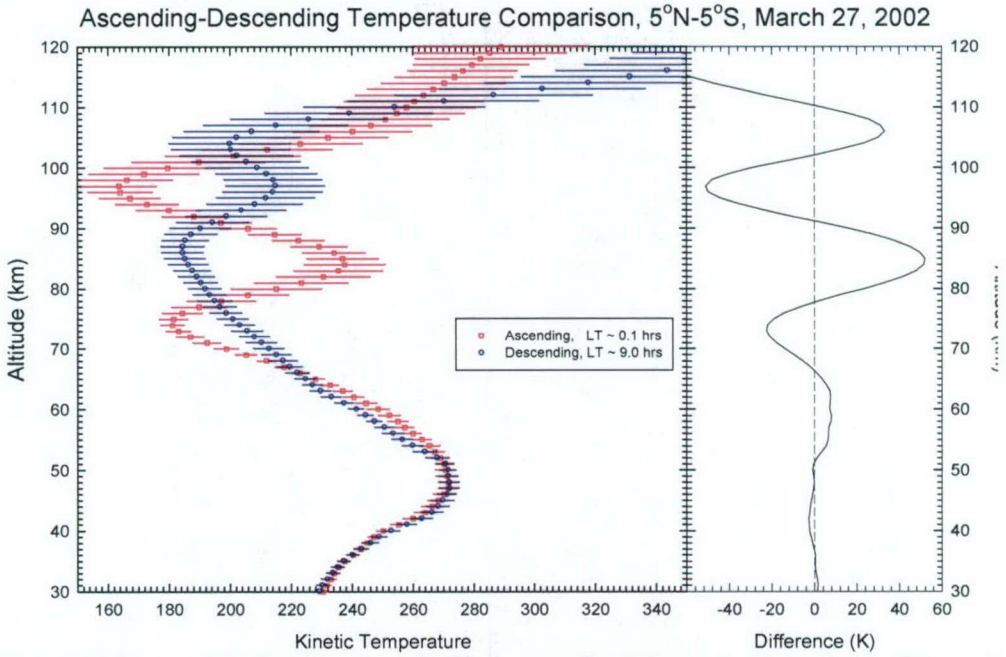

Figure 2. Daily mean kinetic temperatures (T_k) for the ascending (45 events) and descending (47 events) portions of the orbits, and the difference of the two, at the equator for a single day in March 2002, from the Level 2A retrieved T_k values. The error bars give the daily rms deviation.

3. GLOBAL SURVEYS OF RADIANCE AND TEMPERATURE-INVERSION LAYERS

We will analyze on a global basis the occurrence and distribution of layer structures in the SABER channels 1-3 Level 1B and Level 2A data. It is noteworthy that the mean temperature profile of Figure 2 shows on the ascending (night) side a TIL with an increase of almost 60 K in ~10 km near 85 km altitude. This is typical of equinox conditions in the SABER data set. TILs are found in a large fraction of all scans, particularly near the mesopause and at low latitudes. These TILs will sometimes be associated with corresponding radiance layers, or so-called "knees". Moreover, it is very common to have radiance knees at higher altitude in the lower thermosphere, where they are not necessarily associated with local TILs.

Both an initial survey of SABER Level 1B data and earlier investigations of MSX limb data[33] showed that these radiance knees are extremely variable and suggested the value of examining the global occurrence rates of these common but poorly understood features. It turns out that the knees have a distinct LT and latitude dependence. An example is given in Figure 3. The radiance and temperature layers are extremely important for the MLT energy budget, because CO_2 15-μm emission is the dominant cooling mechanism in the lower thermosphere and reaches a maximum there. Atomic oxygen is largely responsible for exciting the 15-μm radiating ν_2 states above 90 km, but prominent knees cannot be reproduced using standard climatologies, even with extremely high O densities. Moreover, variability of atomic oxygen alone is insufficient to explain their appearance, or lack of appearance, and the differences in their

properties. In fact, it is not known reliably why they appear at some times and places, but not at others, although the temperature gradient seems to play a role.

To better understand the radiance knees and to determine their occurrence probabilities and properties, we examined two full yaw cycles (Mar-May and Sep-Nov 2002). Defining knees by the criterion that the ratio R_{max}/R_{min} be greater than 1.1, where R_{max} and R_{min} are the radiances at the two local extrema, we found that these features are clustered along the equator at certain LTs and at midlatitude at other LTs. Figure 4 shows the distribution for the later yaw period in 2002, obtained using 1-h local time and 2° latitude bins. The results are similar for the earlier period. The clustering pattern does not change when the selection criterion is relaxed so as to include events with ratios smaller than 1.1, or strengthened to exclude all ratios below 1.2 or 1.3. We also found that the mean altitude of the radiance maximum varies systematically, as shown for the same yaw period in Figure 5.

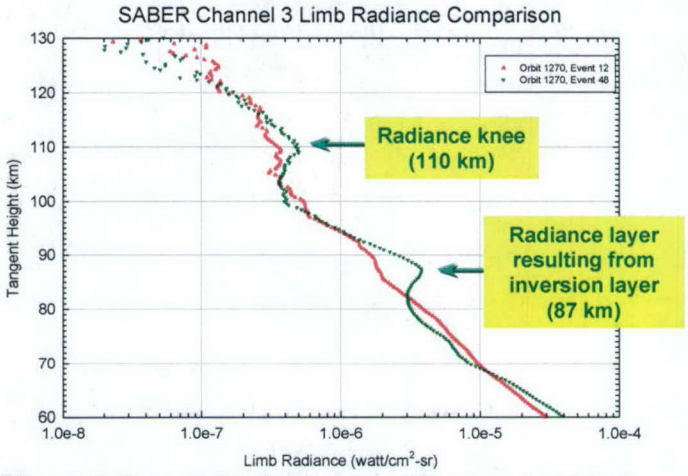

Figure 3. Radiance profiles from two very different events, 3 March 2002. The low-latitude event (7S) shows two layers; the midlatitude event (46N) has none.

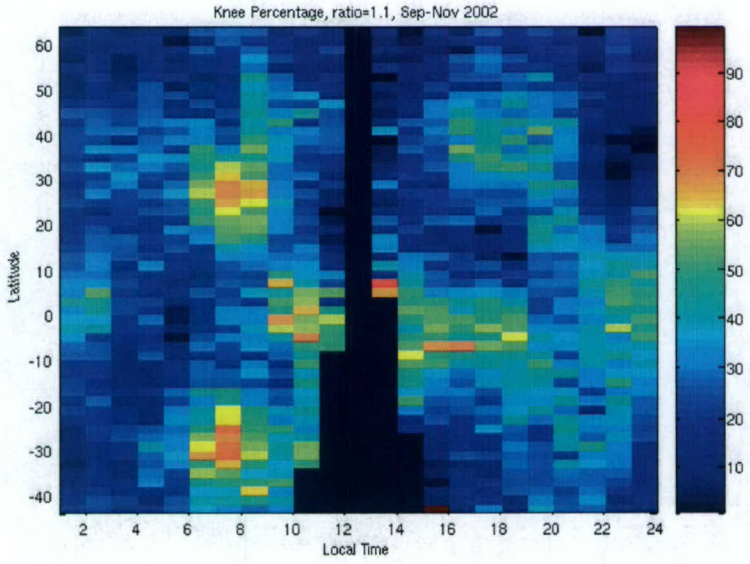

Figure 4. Radiance "knee" occurrence probability distribution for Sep-Nov 2002. The percent of scans with knees is given as a function of latitude and local time. No data are available near local noon.

In Figure 5 in particular, there appears to be a diurnal dependence at the equator, and a semidiurnal dependence at midlatitudes, suggesting some association with tides. Figure 6 shows the altitude of individual radiance knees in the equatorial zone, also suggesting an association with the DT. The exact mechanism whereby the tides may cause these patterns is not yet understood. Considering that atomic oxygen alone does not appear to offer a satisfactory explanation, it is our view that tide-associated variability in the temperature and minor-species profiles in this region may be responsible. However, this remains a work in progress, and model calculations will likely be required to assess the validity of any hypothesis.

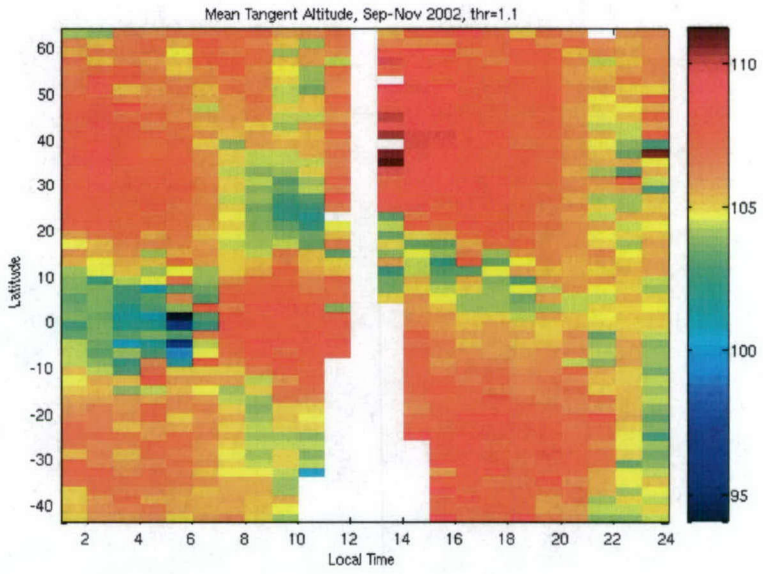

Figure 5. Distribution of mean tangent altitude (km) for radiance "knees", Sep-Nov 2002.

Turning our attention back to the TILs, many Rayleigh lidar studies have shown that TILs are very common in the lower mesosphere near 60 km (for example[34-36]). With the advent of Na resonance lidars it has become clear that there is also an important population of TILs in the mesopause region near 85-90 km.[37-40] The lidar data have shown that many of these layers ,descend in synchrony with the tidal vertical phase motion (for example[41]). In addition, studies with spatially separated lidars have shown that these layers can extend over several hundred km. SABER level 2A data offers the opportunity to do the first global survey of MLT TILs, determine their spatial extent and persistence time, and develop a global climatology of their occurrence and properties.

Figure 6. Altitude of radiance knees for individual events within 10 degrees of the equator, as a function of local time. Data are from the Mar-May 2002 yaw cycle.

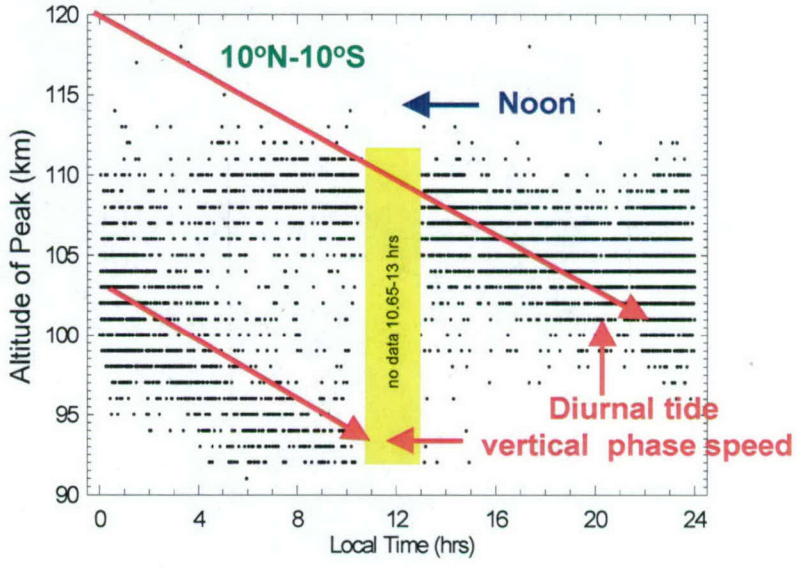

Although a complete theory of TILs is lacking, they seem to be manifestations of lower-atmospheric forcing. It has been suggested that TIL formation can be the result of GW steepening and GW-tidal interactions near critical levels (for example[17,22,42,24]) and also of breaking planetary waves in the mesospheric surf zone.[23-24] It has also been suggested that they are sometimes associated with heat release in exothermic O_x-HO_x reactions.[43] These layers are important to atmospheric energetics because these dynamical-chemical interactions change the form of energy and also because layers radiate much more strongly than the background atmosphere and, hence, influence radiative cooling.

Significant results from the initial phases of our study include the following: (1) TILs are truly large-scale, if not global phenomena, capable of extending coherently for several thousand km along the TIMED satellite track; (2) there is a high probability of finding TILs in the 70-100 km region in any given scan, particularly at night; and (3) many TILs have very large amplitude, much larger than typical predicted tidal amplitudes, even approaching 100 K. Moreover, we have determined their occurrence probability and altitude distribution as a function of latitude and LT.

We have obtained coincidences between SABER and Colorado State University (CSU) lidar[41] measurements of TILs showing both good agreement and the spatially extensive nature of the layers. Figure 7 compares temperature measurements made on 7 Oct 2002. Lidar results for that night recorded a large TIL that persisted for at least eight hours, moving downwards from ~93 km to ~85 km at a rate consistent with the tidal vertical phase speed of ~1 km/hr. Clouds obscured the lidar's view at the time of the SABER overpass, but as shown in the figure the closest measurement in time, 48 minutes later, agreed well with the SABER profiles despite the LOS averaging inherent in the limb retrieval. Moreover, SABER saw TILs in every event of that particular orbit between 61N and 7N, an along-track distance of

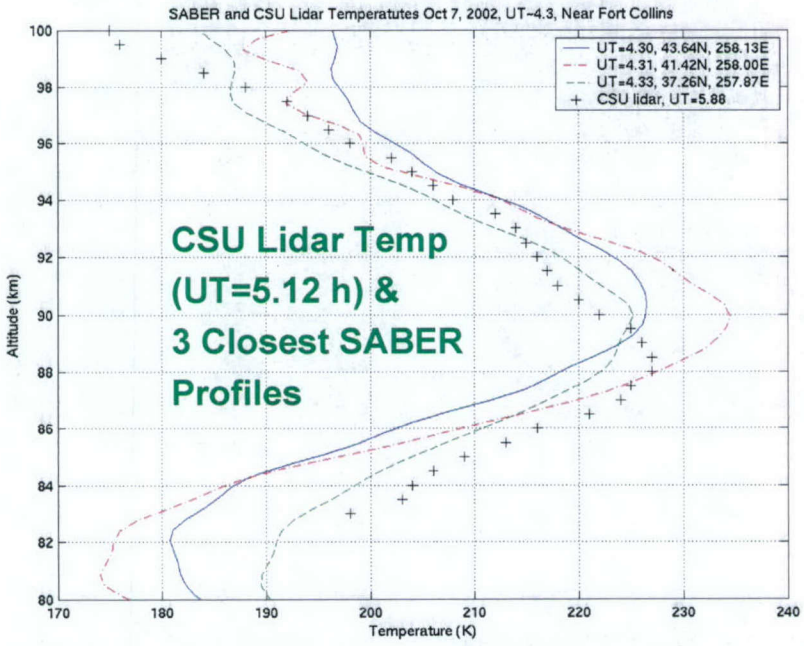

Figure 7. CSU lidar temperature measurements, 7 Oct 2002, compared with the three SABER events that were most nearly co-located.

nearly 6000 km. For the twelve events around the Fort Collins overpass, an along-track distance of 4100 km, the altitude of the TIL was always between 88 and 91 km, very similar to the lidar result. TILs have been seen in groups of consecutive SABER events at many times and locations, giving a good indication that these features are commonly spatially extended in the horizontal direction.

Figure 8 gives the occurrence probability distribution for the Sep-Nov 2002 yaw cycle in much the same fashion as was done above for the radiance knees. Using the Level 2A data, and considering only inversions of at least 20 K, we find TILs in 80-90% of all events in some regions of the latitude/LT space. If the threshold is reduced to 10K, they are nearly ubiquitous in these same regions, which are mostly nighttime. On the other hand, in other regions, the chances of seeing a large inversion are quite small. This is particularly true during daytime at high latitude and midlatitude.

Above, in Figure 2, we saw an inversion of 60 K in the nighttime-mean of the ascending temperature for a single day, near the equator. We identified several individual events with TILs of amplitude 90 K. The largest such features cluster near the equator; in fact, rather few "small" (<20K) TILs are found there near local midnight.

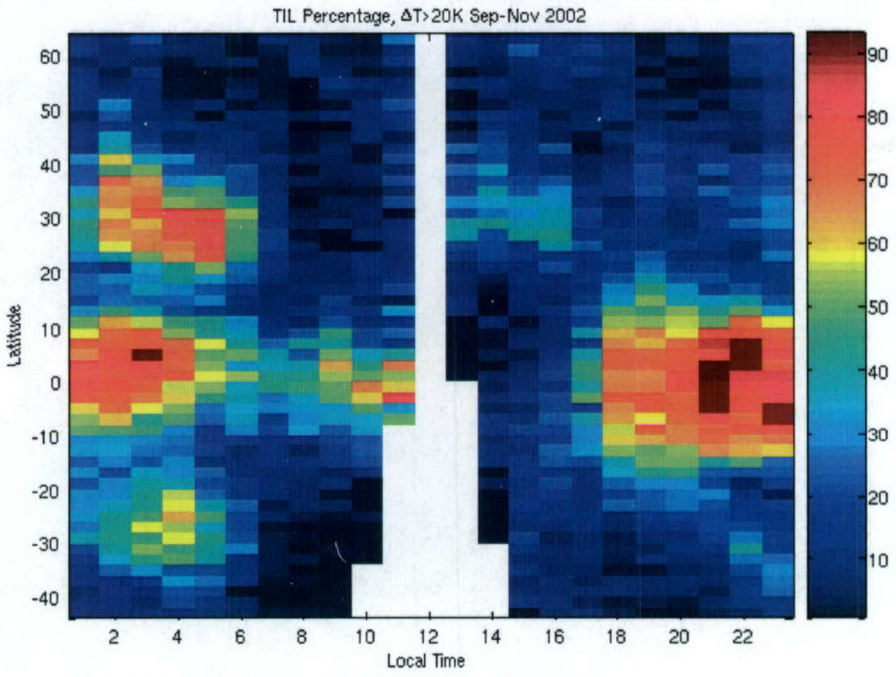

Figure 8. Percentage of all scans in which at least one inversion layer exceeding 20 K was identified, as a function of latitude and local time for the Sep-Nov 2002 yaw cycle.

Figure 9 gives the altitude distribution of all TILs exceeding 20K in the same yaw cycle. In the equatorial region, the layers cluster around ~83 km at night and ~93 km in the daytime. At midlatitudes, the nighttime TILs are the ones most often seen above 90 km.

4. CONCLUSION

We have shown that the Level 1B SABER CO_2 15-μm radiance data and the Level 2A temperature (T_k) data derived from it have a rich structure as a function of latitude and LT. The results show that these data exhibit strong indications of tidal influence. We have also characterized the occurrence probability and properties of layer structures in the data. Both TILs and radiance layers or "knees" show characteristic structure as a function of altitude, latitude, and LT, with

tidal connections well in evidence. Both radiance and T_k layers have a high probability of occurrence, especially in certain regions of space-time, and are spatially extensive. Future investigations will extend this study to other seasons, quantify more thoroughly the spatial correlations and persistence of layer structures, and study in depth whether existing non-LTE radiative theory can explain the radiance knees.

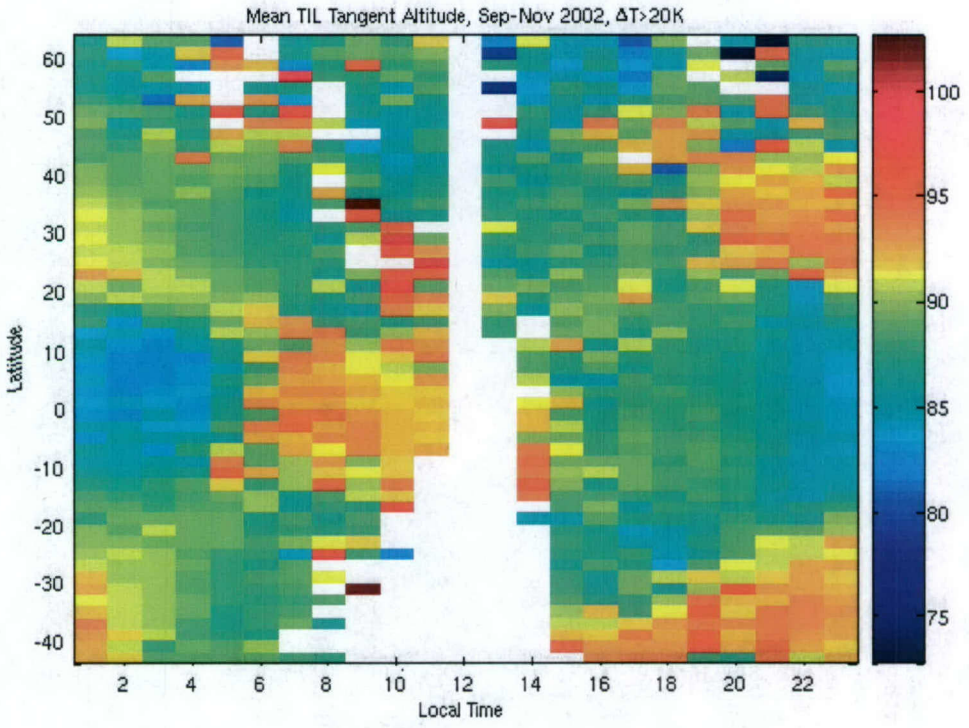

Figure 9. Distribution of inversion-layer altitude (km), Sep-Nov 2002, as a function of latitude and local time.

ACKNOWLEDGEMENTS

RHP, PPW, and JRW are grateful to Kent Miller of the Air Force Office of Scientific Research for partial support of this work. We also acknowledge the support of the NASA Langley SABER program office.

REFERENCES

1. Russell, J.M. III, M.G. Mlynczak, L.L. Gordley, J. Tansock, and R. Esplin, An overview of the SABER experiment and preliminary calibration results, *Proc. SPIE, 3756*, 277-288, 1999.
2. Yee, J.-H., G. E. Cameron, D. Y. Kusnierkiewicz, Overview of TIMED, Proc. SPIE, 3756, 244, 1999.
3. Mertens, C. J., M. G. Mlynczak, M. Lopez-Puertas, P.P. Wintersteiner, R. H. Picard, J. R. Winick, L. L. Gordley, and J. M. Russell III, Retrieval of mesospheric and lower thermospheric kinetic temperature from measurements of CO_2 15 μm Earth limb emission under non-LTE conditions, *Geophys. Res. Lett., 28*, 1391-1394, 2001.
4. Mertens, C. J., M. G. Mlynczak, M. Lopez-Puertas, P. P. Wintersteiner, R. H. Picard, J. R. Winick, L. L. Gordley, and J. M. Russell III, Retrieval of kinetic temperature and chemical abundances from nonlocal thermodynamic equilibrium limb emission measurements made by the SABER experiment on the TIMED satellite, *Proc. SPIE, 4882*, 162-171, 2003.
5. Mertens, C. J., F. J. Schmidlin, R. A. Goldberg, E. E. Remsberg, W. D. Pesnell, J. M. Russell III, M. G. Mlynczak, M. Lopez-Puertas, P. P. Wintersteiner, R. H. Picard, J. R. Winick, and L. L. Gordley, SABER observations of

mesospheric temperatures and comparisons with falling sphere measurements taken during the 2002 summer MacWAVE campaign, *Geophys. Res. Lett.*, *31*, L03105, doi:10.1029/2003GL018605, 2004.
6. Hines, C.O., Internal atmospheric gravity waves at ionospheric heights, *Can. J. Phys.*, *38*, 1441-1481, 1960.
7. Taylor, M. J., and M. A. Hapgood, Identification of a thunderstorm as a source of short period gravity waves in the upper atmospheric nightglow emissions, *Planet. Space Sci.*, *36*, 975-985, 1988.
8. Makhlouf, U. B., R. H. Picard, and J. R. Winick, Photochemical-dynamical modeling of the measured response of airglow to gravity waves 1. Basic model for OH airglow, *J. Geophys. Res.*, *100*, 11,289-11,311, 1995.
9. Dewan, E. M., R. H. Picard, R. R. O'Neil, H. A. Gardiner, J. Gibson, J. D. Mill, E. Richards, M. Kendra, and W. Gallery, MSX satellite observations of thunderstorm-generated gravity waves in mid-wave infrared images of the upper stratosphere, *Geophys. Res. Lett.*, *25*, 939-942, 1998.
10. Picard, R. H., R. R. O'Neil, H. A. Gardiner, J. Gibson, J. R. Winick, W. O. Gallery, A. T. Stair, Jr., P. P. Wintersteiner, E. R. Hegblom, and E. Richards, Remote sensing of discrete stratospheric gravity-wave structure at 4.3-μm from the MSX satellite, *Geophys. Res. Lett.*, *25*, 2809-2812, 1998.
11. Chapman, S., and R. S. Lindzen, *Atmospheric Tides*, Gordon and Breach Science Publishing, New York, 1987.
12. Hagan, M. E., J. M. Forbes, and F. Vial, On modeling migrating solar tides, *Geophys. Res. Lett.*, *22*, *893*-896, 1995.
13. Hagan, M. E., Comparative effects of migrating solar sources on tidal signatures in the middle and upper atmosphere, *J. Geophys. Res.*, *101*, 21,213-21,222, 1996.
14. Hagan, M. E., C. McLandress, and J. M. Forbes, Diurnal tidal variability in the upper mesosphere and lower thermosphere, *Ann. Geophys.*, *15*, 1176-1186, 1997.
15. Walterscheid, R. L., Inertio-gravity wave induced accelerations of mean flow having an imposed periodic component: Implications for tidal observations in the meteor region, *J. Geophys. Res.*, *86*, 9698-9706, 1981.
16. Hauchecorne, A., M. L. Chanin, and R. Wilson, Mesospheric temperature inversion and gravity wave dynamics, *Geophys. Res. Lett.*, *14*, 935-939, 1987.
17. Huang, T. Y., H. Hur, T. F. Tuan, X. Li, E. M. Dewan, and R. H. Picard, Sudden narrow temperature-inversion-layer formation in ALOHA-93 as a critical-layer-interaction phenomenon, *J. Geophys. Res.*, *103*, 6323-6332, 1998.
18. Liu, H.-L., and M. E. Hagan, Local heating/cooling of the mesosphere due to gravity wave and tidal coupling, *Geophys. Res. Lett.*, *25*, 2941-2944, 1998.
19. Liu, H.-L., Temperature changes due to gravity wave saturation, *J. Geophys. Res.*, *105*, 12,329-12,336, 2000.
20. Liu, H.-L., M. E. Hagan, and R. G. Roble, Local mean state changes due to gravity wave breaking modulated by the diurnal tide, *J. Geophys. Res.*, *105*, 12,381-12,396, 2000.
21. Meriwether, J. W., and C. S. Gardner, A review of the mesosphere inversion layer phenomenon, *J. Geophys. Res.*, *105*, 12,405-12,416, 2000.
22. Huang, T. Y., M. P. Hickey, T. F. Tuan, E. M. Dewan, and R. H. Picard, Further investigations of a mesospheric inversion layer observed in the ALOHA-93 Campaign, *J. Geophys. Res.*, *107*, 4408, doi:10.1029/2001JD001186, 2002.
23. Sassi, F., R. R. Garcia, B. A. Boville, and H. Liu, On temperature inversions and the mesospheric surf zone, *J. Geophys. Res.*, *107*, 4380, doi:10.1029/2001JD001525, 2002.
24. Meriwether, J. W., and A. J. Gerrard, Mesosphere inversion layers and stratosphere temperature enhancements, *Rev. Geophys.*, *42*, RG3003, doi:10.1029/2003RG000133, 2004.
25. Fritts, D. C., B. P. Williams, C. Y. She, J. D. Vance, M. Rapp, F.-J. Luebken, A. Muellemann, F. J. Schmidlin, and R. A. Goldberg, *Geophys. Res. Lett.*, *31*, L24S06, doi:1029/2993GL019389, 2004.
26. Sharma, R. D., and P. P. Wintersteiner, Role of carbon dioxide in cooling planetary thermospheres, *Geophys. Res. Lett.*, *17*, 2201-2204, 1990.
27. Wintersteiner, P. P., R. H. Picard, R. D. Sharma, J. R. Winick, and R. A. Joseph, Line-by-line radiative excitation model for the non-equilibrium atmosphere: Application to CO_2 15-μm emission, *J. Geophys. Res.*, *97*, 18,083-18,117, 1992.
28. Lopez-Puertas, M., and. F. W. Taylor, *Non-LTE Radiative Transfer in the Atmosphere*, World Scientific, Singapore, 2001.
29. Zhang, S.-P., and G. G. Shepherd, The influence of the diurnal tide on the $O(^1S)$ and OH emission rates observed by WINDII on UARS, *Geophys. Res. Lett.*, *26*, 529-532, 1999.
30. Ward, W. E., J. Oberheide, M. Riese, P. Preusse, and D. Offermann, Tidal signatures in temperature data from CRISTA 1 mission, *J. Geophys. Res.*, *104*, 16,391-16,403, 1999.
31. Ward, W. E., A simple model of diurnal variations in the mesospheric oxygen nightglow, *Geophys. Res. Lett.*, *26*, 3565-3568, 1999.

32. Shepherd, M. G., W. F. J. Evans, G. Hernandez , D. Offermann , and H. Takahashi, Global variability of mesospheric temperature: 1. Mean temperature field, *J. Geophys. Res.*, in press, 2004.
33. Picard, R. H., J. R. Winick, and P. P. Wintersteiner, Non-equilibrium radiative transfer in structured atmospheres, *Proc. SPIE, 4539*, 454-468, 2001.
34. Hauchecorne, A., and M. L. Chanin, Density and temperature profiles obtained by lidar between 35 and 70 km, *Geophys. Res. Lett., 7*, 565-668, 1980.
35. Hauchecorne, A., M.-L. Chanin, and P. Keckhut, Climatology and trends of the middle atmospheric temperature (33-87 km) as seen by Rayleigh lidar over the south of France, *J. Geophys. Res., 96*, 15,297-15,309, 1991.
36. Fiedler, J., G. Baumgarten, G. von Cossart, and A. Schoech, Lidar observations of temperatures, waves, and noctilucent clouds at 69° N, *Proc. SPIE, 5571*, this issue, 2005.
37. She, C. Y., H. Lafiti, J. R. Yu, R. J. Alvarez II, R. E. Bills, and C. S. Gardner, Two-frequency lidar technique for mesospheric Na temperature measurements, *Geophys. Res. Lett., 17*, 929-932, 1990.
38. Bills, R. E., C. S. Gardner, and C. Y. She, Narrowband lidar technique for sodium temperature and Doppler wind observations of the upper atmosphere, *Opt. Eng., 30*, 13-21, 1991.
39. Dao, P. D., R. Farley, X. Tao, and C. S. Gardner, Lidar observations of the temperature profile between 25 and 103 km: Evidence of tidal perturbation, *Geophys. Res. Lett., 22*, 2825-2828, 1995.
40. States, R. J., and C. S. Gardner, Thermal structure of the mesopause region (80ñ105 km) at 40 N latitude. Part II: Diurnal variations, *J. Atmos. Sci., 57*, 78-92, 2000.
41. She, C. Y., T. Li, B. P. Williams, T. Yuan, and R. H. Picard, Concurrent OH imager and sodium temperature/wind lidar observation of a mesopause region undular bore event over Fort Collins/Platteville, CO, *J. Geophys. Res.*, in press, 2004.
42. Hur, H., T. Y. Huang, Z. Zhao, P. Karananayaka, and T. F. Tuan, A theoretical model analysis of the sudden narrow temperature-layer formation observed in the ALOHA-93 Campaign, *Can. J. Phys., 80*, 1543-1558, 2002.
43. Meriwether, J. W., and M. G. Mlynczak, Is chemical heating a major cause of the mesosphere inversion layer?, *J. Geophys. Res., 100*, 1379-1387, 1995.